DC Josephson Effect and Andreev Bound States in Superconductor-Normal Metal-Superconductor Junctions

Reet Santosh Mhaske[1]

Guide: Prof. Bhaskaran Muralidharan[2]

20D170032, [1]Department of Physics, Indian Institute of Technology, Bombay

[2]Department of Electrical Engineering, Indian Institute of Technology, Bombay

I. INTRODUCTION

Josephson Junctions have played a critical role in the field of superconducting devices. Besides being the fundamental unit of the superconducting qubits, it boosted the study of circuit Quantum Electrodynamics. In this report, we study one particular type of Junction, the superconductor-normal metal-superconductor junction, using the Non-Equilibrium Green's function approach. We attempt at recreating the Josephson's first relation.

The flow of the report is as follows. In section II, previous works on modelling Josephson junctions using NEGF are enlisted. Then we start by theoretically introducing superconductivity in section III. Here we review the Nambu space, dispersion relation for superconducting bulk and Andreev bound states. In section III we describe the model that we will be dealing with. In section IV we present the numerical results, the central part of this report. We conclude the report in section VI.

II. IMPORTANT WORKS

Modelling S-N-S junctions has been previously done in Ref[1] and Ref[2]. The study of SNS Junctions in presence of magnetic fields for conducted by Blair and Hampshire Ref [3].In Ref[4], the authors study the proximity effect in planar SNS Junctions. Beyond SNS Junctions, junctions with topological insulators have also been studied.

III. THEORETICAL BACKGROUND

A. SUPERCONDUCTIVITY

The principle insight of the Bardeen-Cooper-Schriefffer Theory (BCS Theory) of Superconductivity was that at sufficiently low temperatures, there exists an attraction between electrons. Depending on the type of the superconductor, this attraction can be mediated by different mechanisms. The primary mechanism we shall deal with is the interaction mediated via phonons. In principle it is possible to account for this interaction by considering the vibrational modes of the lattice while writing the total Hamiltonian, but the essence of the phenomenon can be captured by a much simpler model. We assume that the interaction is represented by a delta attractive potential at each point in space,

$$U(x,x') = -g\delta(x-x') \qquad (1)$$

for a positive g (So that the attraction is positive). This roughly implies that an attractive force exists between two electrons only if they are at the same position in space.

Although crude in its assumption, we can write the BCS Hamiltonian, under the above assumption to be

$$H_{BCS} = -g\int dx[\psi_\uparrow^*(x)\psi_\downarrow^*(x)\psi_\downarrow(x)\psi_\uparrow(x) + \psi_\downarrow^*(x)\psi_\uparrow^*(x)\psi_\uparrow(x)\psi_\downarrow(x)] \qquad \ldots (2)$$

The operator $\psi_\uparrow(x)$ or $\psi_\uparrow^\dagger(x)$ annihilates or creates a fermionic particle at position x of ↑ spin respectively. The Hamiltonian represents the act of two electrons of opposite spins at position x being annihilated and two electrons, of opposite spins, being created at the same position, thus coupling the two electrons.

Using Feynman diagram, the same can be represented as below:

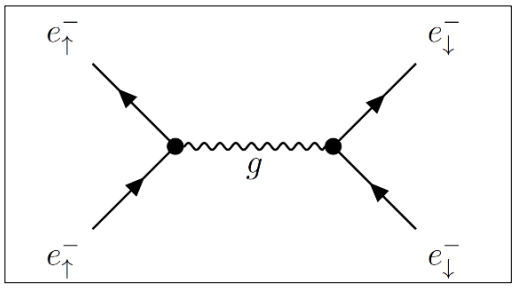

Fig 1. Feynman Diagram for electron interaction. (source: Ref[1])

If we introduce the vector and the Pauli matrix

$$\psi = \begin{bmatrix}\psi_\uparrow \\ \psi_\downarrow\end{bmatrix} \qquad \sigma_2 = \begin{bmatrix}0 & i \\ -i & 0\end{bmatrix} \qquad (3)$$

We can write the Hamiltonian compactly as

$$H_{BCS} = -\frac{g}{2}\int dx\,[\psi^T(x)(i\sigma_2)\psi(x)]^\dagger\;[\psi^T(x)(i\sigma_2)\psi(x)] \quad (4)$$

This is a quartic Hamiltonian, in which the two electrons of opposite spins are coupled (both are created and annihilated at the same position).

Fig 2. Cooper Pair formation in the two electron picture

Now we use the mean field decoupling approximation to reduce the Hamiltonian to

$$H_{BCS} = -\frac{1}{2}\int dx\,\Delta^*(x)[\psi^T(x)(i\sigma_2)\psi(x)] + [\psi^T(x)(i\sigma_2)\psi(x)]^\dagger\Delta(x) \quad (5)$$

where

$$\Delta(x) = g\langle\psi_\uparrow\psi_\downarrow\rangle - g\langle\psi_\downarrow\psi_\uparrow\rangle \quad (6)$$

$\Delta(x)$ is called the gap parameter, which can be complex. In the mean field approximation, we have neglected a term of $|\Delta|^2$, which can be accounted for in the chemical potential.

To model a superconducting bulk, we can take the Δ to be independent of x and have $\Delta = |\Delta|e^{i\phi}$

The Hamiltonian in equation(5) has terms of form $\int dx\,\Delta^*\psi_\uparrow\psi_\downarrow$, which are quadratic in nature.

This denotes two electrons being destroyed at the location x. This annihilation of two electrons in turn results in creation of a "Cooper pair" of

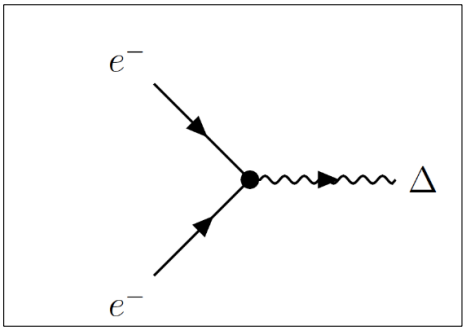

Fig 2. Cooper Pair formation in the electron -electron picture. (source: Ref[1])

electrons. A Cooper Pair can be thought of as a Boson formed by the coupling of two electrons with opposite spins. This creation of Cooper Pairs can be represented using Feynman Diagram[Fig2]

Now, an electron with momentum $+k$ corresponds to the motion of an imaginary particle (or a "hole"), with momentum $-k$.

We can think of the hole as a vacancy (rather unoccupancy) of an energy state. This argument then justifies another equivalent picture of creation of Cooper Pairs, where in an electron gives rise to a Cooper Pair and a hole, as shown in Fig 3.

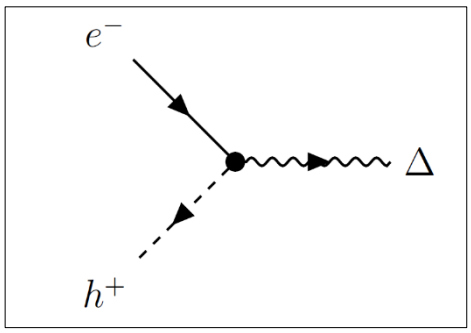

Fig 3. Cooper Pair formation in the electron -hole picture. (source: Ref[1])

We can therefore identify ψ^* as the wave function of the hole, and define the 4-component Nambu spinor to be $\Psi(x) = \begin{bmatrix}\psi(x)\\ \psi^*(x)\end{bmatrix}$ so that we simply the Hamiltonian into

$$H_{BCS} = -\frac{g}{2}\int dx\,\Psi^T(x)\begin{bmatrix}0 & \Delta i\sigma_2\\ (\Delta^* i\sigma_2)^\dagger & 0\end{bmatrix}\Psi^*(x) \quad (7)$$

Having discussed the general formalism of Hamiltonian in BCS, we now study the energy spectrum of a superconducting bulk.

B. ENERGY SPECTRUM OF SUPERCONDUCTING BULK

We now consider a superconducting bulk and find the dispersion relation for the same. The Hamiltonian of the bulk in momentum space is be given by

$$H = \Sigma_k\left(\frac{\hbar^2k^2}{2m_e}-\mu\right)\Psi_{k\uparrow}^\dagger\Psi_{k\uparrow} + \left(\frac{\hbar^2k^2}{2m_e}-\mu\right)\Psi_{k\downarrow}^\dagger\Psi_{k\downarrow} - \Delta_o^*\Psi_{-k\downarrow}\Psi_{+k\uparrow} - \Delta_o\Psi_{+k\uparrow}^\dagger\Psi_{-k\downarrow}^\dagger \quad (8)$$

The first two terms denote the free particle energy of the electrons. The last two terms denote the coupling of the electrons as discussed earlier.

We can now introduce the 2-component Nambu spinor, given by

$$\Psi_k = \begin{bmatrix}\psi_{k\uparrow}\\ \psi_{-k\downarrow}^*\end{bmatrix} \quad (9)$$

The justification for identifying $\psi_{-k\downarrow}^*$ as the annihilation operator of a hole follows similar arguments as before. Defining $\xi_k = \frac{\hbar^2k^2}{2m} - \mu$, we can simplify the Hamiltonian as

$$H_{BCS} = \Sigma_k \Psi_k^\dagger \begin{bmatrix} \xi_k & -\Delta \\ -\Delta & -\xi_k \end{bmatrix} \Psi_k^* \quad (10)$$

On diagonalizing, we get the eigenenergy corresponding to the wavevector k to be

$$E(k) = \pm\sqrt{\Delta^2 + \xi_k^2} \quad (11)$$

We see that there are two branches of the dispersion relation, separated by an energy gap of 2Δ. This is because to create an excitation we need to break a Cooper Pair, which would require an energy corresponding to Δ_o. We plot the dispersion relation below for $\mu = 30\Delta_o$ and $\mu = 3\Delta_o$. We observe that the around the fermi energy. the dispersion is almost linear.

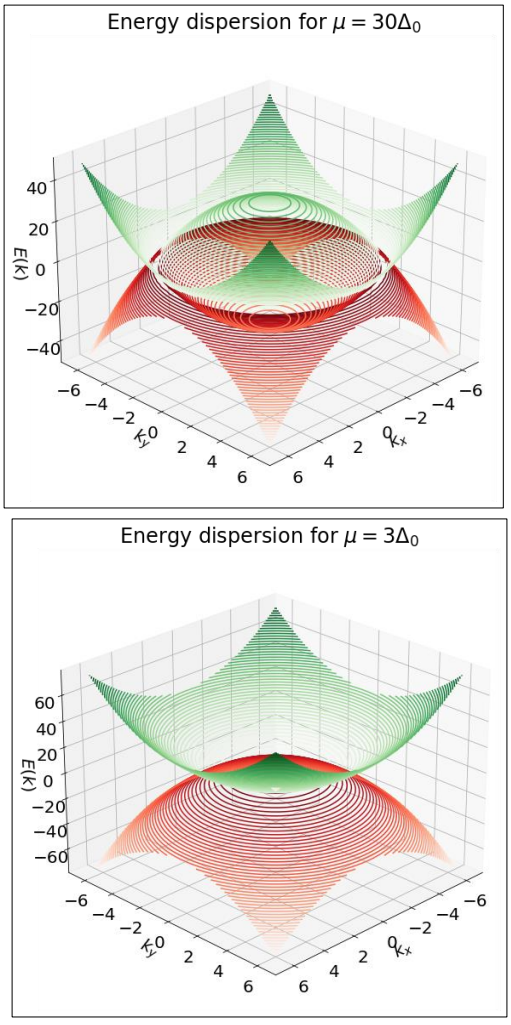

Fig 4. Dispersion Relation of superconducting bulk for different chemical

C. ANDREEV BOUND STATES

Consider a system with a normal metal sandwiched between two semi-infinite superconductors. We can show that for an electron travelling from the normal metal side towards the superconductor interface the change in the absolute value of its momentum is approximately $\delta p \sim p_F \frac{\Delta}{\mu}$. For most materials, it is reasonable to take $\mu \gg \Delta$, in which the change in magnitude of momentum is 0. This is known as the Andreev approximation

If the electron's energy E > Δ, the incident electron can either be reflected back into the normal metal or transmitted into the superconductor, with the transmission probability increasing with increase in E. However if E< Δ , there are no empty states available in the superconductor, so the electron must reflected back as a hole, having transmitted a Cooper Pair into the Superconductor. The same process can reverse itself at the other interface, with the hole being reflected as an electron.

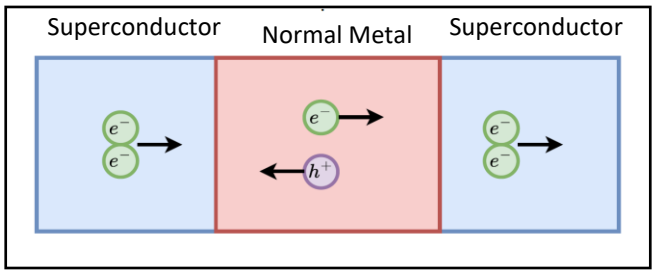

Fig 5. Schematic of Andreev Reflections in SNS Junction

These reflections are known as **Andreev Reflections.** These multiple Andreev Reflections cause a dissipation-less current to flow between the superconducting terminals. It must be noted that the normal metal could not otherwise support the transmission of Cooper Pairs.

III. THE S-N-S JUNCTION

In the previous section we saw how a S-N-S junction can support Andreev States. In this Section we will present the setup that we will be studying.

We shall consider a 1-D junction, with semi-infinite superconducting leads. In the Nambu representation, we can represent the onsite terms of the Hamiltonians in the Superconductor (α_S) and Normal Metal (α_N) part are given by

$$\alpha_S = \begin{bmatrix} 2t-\mu & \Delta \\ \Delta^* & -2t+\mu \end{bmatrix}; \alpha_N = \begin{bmatrix} 2t-\mu & 0 \\ 0 & -2t+\mu \end{bmatrix}$$

Thus, in both the media, the electron and hole parts of the "quasiparticle" each have a self energy term (given by the diagonal elements). 't' denotes the transmission coefficient. In the Superconductor there are interactions between the electron and the hole part (the off-diagonal elements) which are absent in the normal metal.

For both the media, assuming the same effective mass, we write the transmission matrix in the Nambu notation as

$$\beta = \begin{bmatrix} -t & 0 \\ 0 & t \end{bmatrix}$$

The complete Hamiltonian of the Normal metal part is then given in the Nambu space as

$$H = \begin{pmatrix} \alpha_N & \beta & 0 & \cdots & 0 \\ \beta^\dagger & \alpha_N & \beta & \vdots & \vdots \\ 0 & 0 & 0 & \cdots & \alpha_N \end{pmatrix} \qquad (22)$$

The Δ appearing in the onsite terms of the superconductor can be complex. We let $\Delta_R = \Delta_o$ and $\Delta_R = \Delta_o e^{i\phi}$, i.e. let ϕ be the phase difference between the gap parameters between the two superconducting contacts. This is summarized in Fig 5.

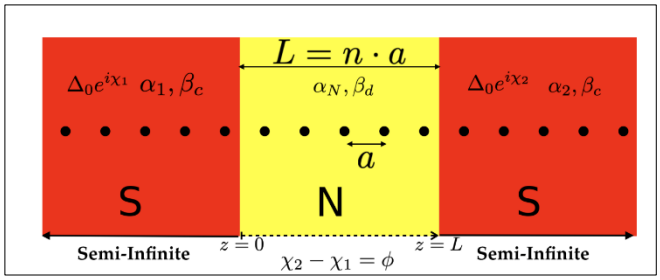

Fig 5. Schematic of SNS junction and the Hamiltonian parameters (source: Ref[2])

IV. Numerical Results

The Green's function for the normal metal part is found using

$$G = (EI - H - \Sigma_r - \Sigma_l)^{-1} \qquad (23)$$

where $\Sigma_{r(l)}$ are the self-energies of the right(left) contact. The self-energies of the contact are found using the Green's function of the superconducting terminals which in turn are found using the recursive Green's Function technique described in the appendix of reference [2].

A. Density of States

The plot below denotes the density of states available at different energies for different phase differences, for $\mu = 30\Delta_o$. We see that there are singularities at certain energies for a particular value of phase difference. These are the energy levels that correspond to the Andreev Bound states. We have highlighted these energy levels in white. We see there are two "branches" which intersect at $\phi = \pi$. We will show in the later sections that the branch starting from below corresponds to electrons and the branch starting from above corresponds to holes.

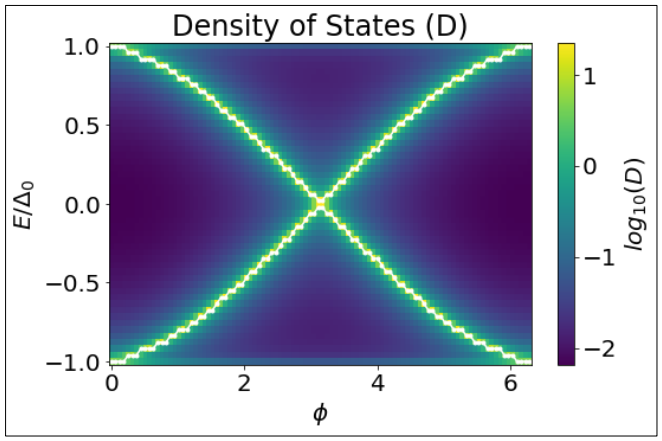

Fig 6. Density of states for SNS junction at $\mu = 30\Delta_o$

B. Introducing Scatterers

We now introduce a scattering potential halfway between the normal metal, by introducing a delta potential. This is achieved by adding an offset U_o to the self-energy terms at the corresponding lattice site.

For a non-zero scattering potential, we see that the cross-over of the two branches is "avoided"

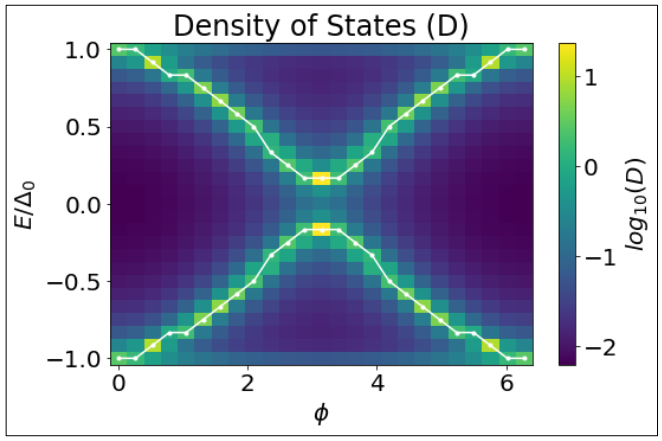

Fig 7. Density of states for SNS junction with a finite scattering potential

We can show analytically that for a given delta potential that scales as U_o, the intensity transmission coefficient is given by

$$T_r = \left(1 + \left(\frac{U_o}{\hbar v_F}\right)^2\right)^{-1}$$

Where v_F is the fermi velocity. We assume U_o to be scaled in the appropriate units and shall take $(1 + (U_o)^2)^{-1}$ to be a measure of transmission coefficient. We plot the DOS for different values U_o below. We observe that the energy difference

between the ABS states increases with more scattering. (Fig 8)

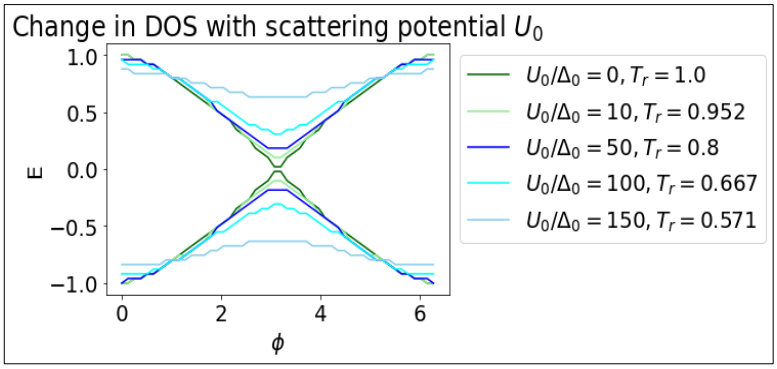

Fig 8. Density of states for SNS junction with changing scattering potential

C. Current

We can find the current using the NEGF technique described.

First consider the relation between DOS and current for a particular phase difference in Fig 9

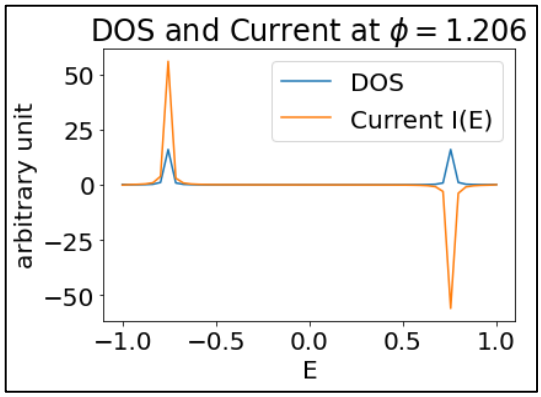

Fig 9. Correlation between DOS and current, both plotted on the same axis (arbitrary units)

We see that the state with negative energy level contributes to a positive current and that with positive energy contributes to negative current. The total current at 0K would be dominated only by the negative energy states, as the hole energies lie above the fermi energy (at E=0). Now, for $\phi < \pi$, the negative energy states correspond to electrons and for $\phi > \pi$, to holes. Hence at $\phi = \pi$, we expect a change in the sign of the current, as

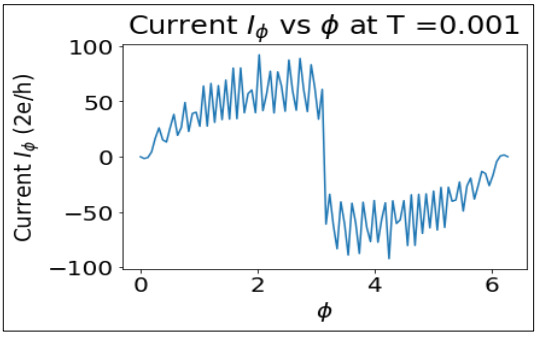

Fig 10. Current vs Phase relation at 0K

the type of carrier dominating the current changes.

We observe the expected trend in the current vs phase relation.

If we increase the temperature, we expect to see a decrease in the net current , since the second branch in the DOS starts getting filled, which contributes to current in the opposite direction.

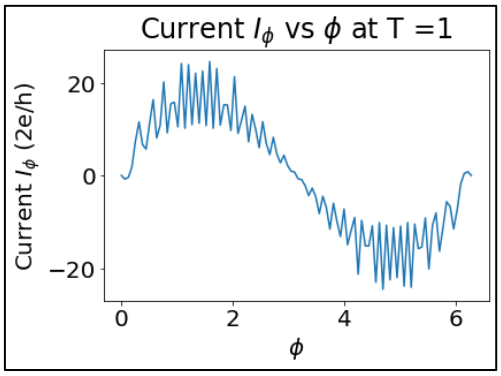

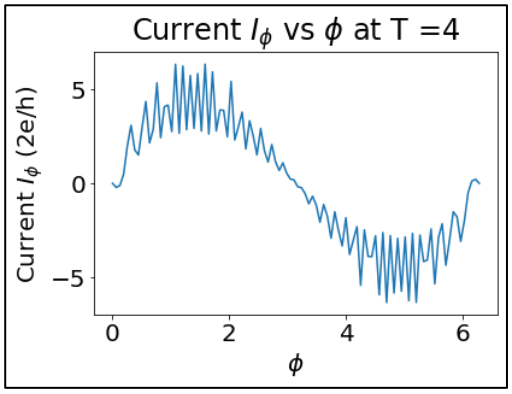

Fig 11. Current vs Phase relation at higher temperatures

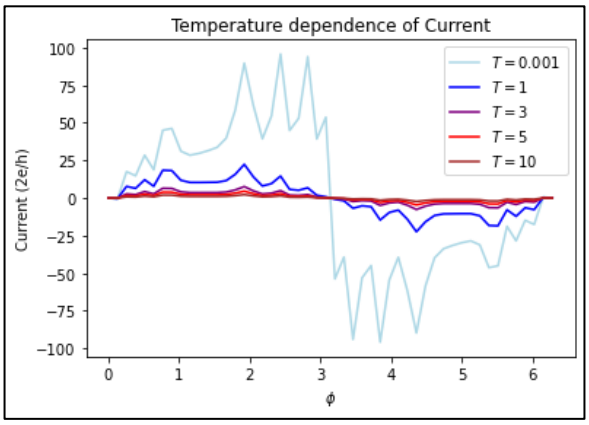

Fig 12. Current vs Phase relation over a range of temperatures

Besides a decrease in the net current, we observe that the relation approaches a sinusoidal one, i.e $I \propto \sin(\phi)$. This is the **Josephson's first relation.** The noisy peaks in the currents are attributed to the finiteness of our discretization model and to the algorithmic limitations. A complete picture of how temperature affects current can be seen in Fig 12.

D. Energy Gap in the ABS states

Even in a junction without scatterer, the DOS changes when we decrease the chemical potential μ so that it is comparable to Δ_o. Below we plot the energy gap δ_{ABS} between the two branches at $\phi = \pi$

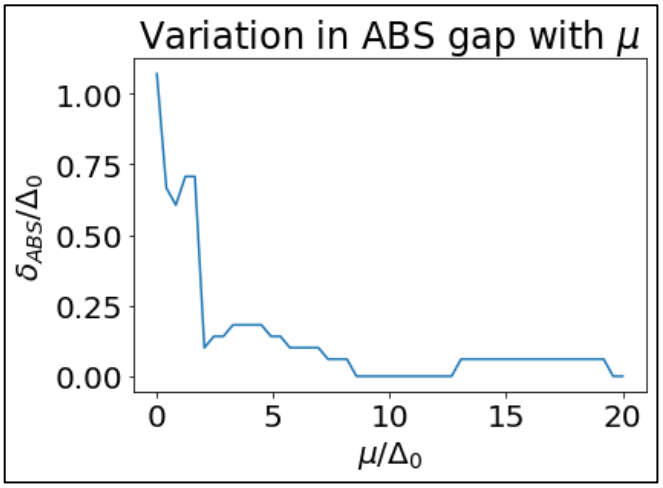

Fig 13. ABS energy gap at $\phi = \pi$ for different μ

We see that beyond the Andreev Approximation, i.e when $\mu \sim \Delta_o$, the two branches have an avoided crossover.

We also plot the energy gap δ_{ABS} at $\phi = \pi$ for a fixed μ and vary the length of the normal metal. We observe that the gap shows oscillations. These can be attributed to the interference of the reflected particles with varying lengths of the normal metal.

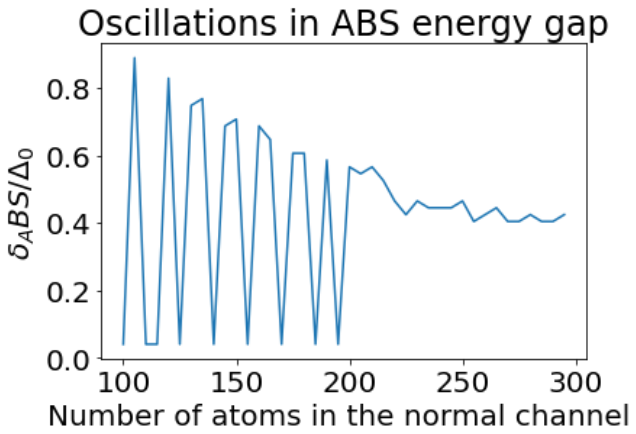

Fig 14. ABS energy gap at $\phi = \pi$ for different number of sites in the normal metal region

V. CURRENT STATUS AND APPLICATION

There have been several proposals to utilize SNS Junctions for qubit implementation. In particular Ref[5] and Ref[6] discuss the experimental applications of the same. It must be noted that the NEGF formalism is being extensively applied to study other types of Josephson Junctions . Ref[7] conducts a study of metal-graphene edge contacts in ballistic Josephson Junctions. In a nutshell, with the advent of superconducting circuit technology for quantum computation, Josephson Junctions are witnessing a renewed interest. This is further extended by the possibility of included novel materials into the setup.

VI. CONCLUSION

We have demonstrated the implementation of NEGF technique to solve for the current and the DOS in a SNS Junction. We saw the effect of scatterers on the DOS of the junction. We then plotted the Andreev current for different temperatures. The results qualitatively follow the relation expected by analytical treatment of the problem. We also saw the oscillations of ABS energy gap with varying length of the normal metal.

VII. ACKNOWLEDGEMENTS

I would like to acknowledge the constant support and valuable guidance of Prof Bhaskaran Muralidharan, also one of the co-authors of Ref[2], which served as a principle reference for this project.

VIII. REFERENCES

1. Quantum Transport in Josephson Junction, Ross D. Monaghan
2. Supercurrent interference in semiconductor nanowire Josephson junctions, P Sriram
3. Critical Current Density of SNS Josephson Junctions and Polycrystalline Superconductors in High Magnetic Fields, Blair and Hampshire
4. .Intrinsic dissipation in superconducting Junctions probed by qubit spectroscopy, Golubev et al
5. Towards n-Parity Protected Superconducting Qubits using 2D Electron Gas, Billy Lim Jun Ming
6. SNS Joesphson Junctions with Tunable Ta-N barriers, Wolak et al
7. First-principles study of metal-graphene edge contact for ballistic Josephson junction, Yeonghun Lee et al

IX. CODE

The self-written code for the simulations is available at the following Github link https://github.com/ReetMhaske/EE755-Project-Code